

RIKER, R.E. and FELLENIUS, B.H., 1992. A comparison of static and dynamic pile test results. Proceedings of the Fourth International Conference on the Application of Stress-Wave Theory to Piles, Ed. F.B.J. Barends, DenHague, September 21-24, 1992, A.A. Balkema, pp. 143-152..

A comparison of static and dynamic pile test results

R. E. Riker
CH2M Hill, Corvallis, Oreg., USA

B. H. Fellenius
University of Ottawa & Anna Geodynamics Inc., Ont., Canada

ABSTRACT During the design of a major bridge across Alsea Bay in Waldport, Oregon, USA, dynamic and static tests were performed on a 40 m long, 510 mm square, prestressed, precast concrete pile, instrumented with strain gages and telltales. The objective of the tests was to determine the maximum design load considering capacity and settlement. The soils consisted of about 40 m of estuarine deposits overlying siltstone bedrock. The presence of a layer of compressible silt directly over the siltstone dictated the use of pile foundations driven to develop a high capacity in the siltstone. An important part of the testing programme was the determination of load distribution in the pile during the static test. The pile was jettted through the upper about 30 m and, then, driven to termination in the siltstone. Dynamic measurements were taken during initial driving and restriking (two days after EOID). A static loading test was carried out ten days after the restriking. A comparison of the results of dynamic and static analyses show that (1) only very little shaft resistance occurred in a jettted zone, (2) the shaft resistance in the lowest soil layer, the silt stratum, was found to be much smaller in the CAPWAP analysis of restrike data than in the analysis of the static test, suggesting incomplete soil set-up at the restriking event, and (3) the toe resistance mobilized in the CAPWAP at a toe movement of about 6 mm (0.23 inch) was much smaller than the toe resistance mobilized in the static loading test at a toe movement of 45 mm.

INTRODUCTION

The Oregon Department of Transportation, State Highways Division, is undertaking a number of major projects to upgrade existing bridges along the Oregon coast Highway. Some of these existing bridges were built in the 1930s and have suffered serious deterioration from corrosion of the reinforcing steel and spalling of the concrete. One such bridge, located over Alsea Bay in Waldport had deteriorated to an extent that replacement of the bridge was necessary.

A new bridge was designed and constructed over a five-year period between 1987 and 1991. The new \$50,000,000 bridge, Fig. 1, includes both reinforced concrete and steel construction. The overall length of the bridge is approximately

915 m (3,000 ft). The approach to the main bridge span includes a series of short, reinforced concrete approach spans, each approximately 60 m (200 ft) in length. The main span is a 150 m long (500 ft) steel arch structure. Both the approach and main span structures are supported on concrete piers founded on piles driven through estuarine deposits and into a siltstone bedrock.

Early in the project design phase, a pile testing programme was conducted to investigate the drivability at the site and suitable design loads. Pile driving tests and static loading tests were conducted over a five-week period in April and May of 1987. One of the piles tested was a spliced, 510 mm (20 inch) square prestressed, precast, concrete pile.

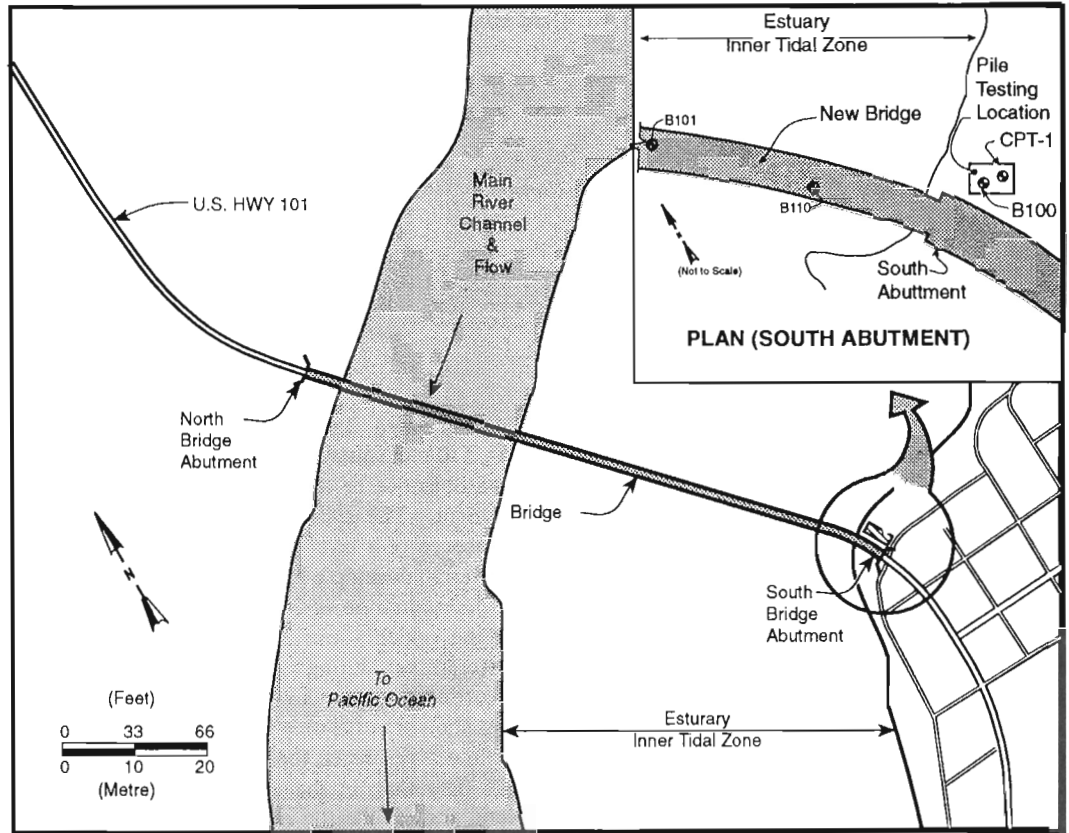


Fig. 1 Site Plan

SOIL PROFILE

The geotechnical exploration programme—completed prior to pile testing—consisted of soil borings, cone penetrometer soundings, and laboratory testing

and revealed a series of estuarine deposits overlying siltstone. Table 1 presents a summary of the depths, thickness, and continuity of the various strata across the site.

TABLE 1. Summary of Soil Conditions

Stratum	Type of Material	Thickness m (ft)	SPT N-value Bl/0.3m	Estimated drained friction angle degrees
1	Fine to medium grained sand with shell fragments, trace silt	10 to 20 (30 to 60)	4 to 25	35
2	Plastic silt and sandy silt (ML)	3 to 10 (10 to 30)	2 to 5	30
3	Silty fine sand and poorly graded sand (SP and SM)	10 to 20 (30 to 60)	6 to 34	38
4	Plastic silt and sandy silt (ML)	6 to 14 (20 to 50)	4 to 6	28
5*)	Silty sand (SM)	20 to 21 (60 to 70)	13 to 25	36
6	Siltstone bedrock	-----	-----	--

The groundwater table varies with tidal fluctuations from near surface to depths of about 3 m (10 ft).

The pore pressure is hydrostatically distributed.

*) The Stratum 5 soil was not present at the location of the pile test.

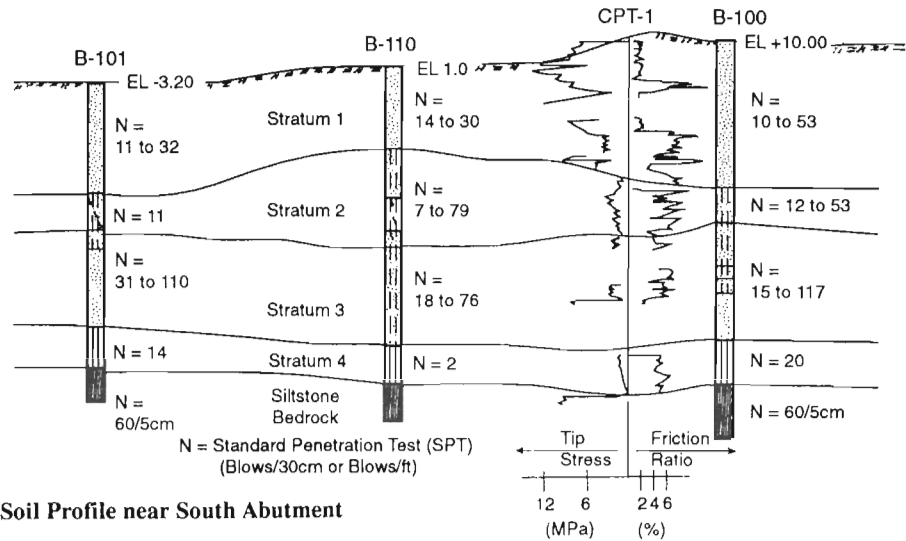


Fig. 2 Soil Profile near South Abutment

Fig. 2 shows a plan view over the test location, the results of soil borings, a cone penetrometer test (CPT) made at the site, and the summarized soil profile.

The presence of the 3 m to 5 m (10 ft to 15 ft) layer of compressible silt directly above the siltstone along with strict structural requirement regarding the magnitude of total and differential settlement precluded the use of shaft bearing piles and dictated placing the bridge foundations on toe bearing piles driven to develop high capacity in the siltstone. Two key aspects of the test programme were therefore:

The maximum practical toe bearing capacity which could be achieved by driving the piles into the siltstone.

The amount of dragload due to negative skin friction that ultimately would be transferred to the neutral plane (located near the pile toe).

PILE TESTING DETAILS

Test Pile and Pile Driving Equipment

The 510 mm (20-inch) concrete pile was composed of two 20.6 m (67.5 ft) long segments that were spliced in the field by means of a mechanical splice type ABB. Each pile segment was cast with a 90 mm diameter (3.5 inch) center

tube to facilitate jetting during installation and to accommodate the strain gages and telltales. The splice was prepared for passage of the center pipe.

The pile was driven by means of a Delmag D46-23 open-end diesel hammer with a nominal energy range of 65 KJ through 142 KJ (48.4 ft-kip through 105 ft-kip). The driving system included a 150 mm (6 inch) aluminum-micarta hammer cushion and a 300 mm (12 inch) oak plywood pile cushion.

The pile driving was monitored in conformance with ASTM D4945 using the Pile Driving Analyzer (Rausche et al., 1985). The initial driving took place on May 6, 1987 and restriking was performed 2 days later, on May 8, 1987.

The first pile segment was installed by jetting through the center tube and out a jet nozzle flush with the pile toe to a depth of 18.6 m (61 ft). The second segment was then aligned and connected to the first by means of the ABB splice, which procedure took approximately 10 minutes. The jetting, supplemented by small gravity drops of the hammer ram, then continued until an embedment depth of 30.5 m (97 ft). Beyond the 30.5 m depth, the pile was advanced by impact driving only, using maximum hammer fuel setting. The driving was terminated at an embedment depth of 38.0 m (124.8 ft), about 0.6 m (2 ft) into the siltstone.

Test Pile Instrumentation

To provide data for estimating load distribution along the pile during the static testing, the test pile was equipped with ten strain gages and two telltales. One telltale was anchored at the toe of the pile to record the movement of the pile toe during the test. The other telltale was 5.9 m (19.5 ft) shorter.

The strain gages were spot-weldable vibrating wire gages placed in pairs at five locations in the center pipe along the pile: at distances up from the pile toe of 1.4 m, 4.4 m, 7.5 m, 10.5 m, 13.8 m, 35.2 m (4.5 ft, 14.5 ft, 24.5 ft, 34.4 ft, 45.4 ft, and 115.6 ft). The telltales consisted of 6.4 mm (1/4 inch) diameter, solid extensometer rod with flush coupled connections placed inside I.D. 9.5 mm (3/8 inch) guide pipes. The lengths of the telltales were 30.85 m and 36.80 m (101.23 ft and 120.72 ft). Fig. 3 shows the arrangement of the strain gages and telltales. The uppermost strain-gage pair (No. 6) ceased to function at the applied load of 5,100 kN (575 tons), but the other gage pairs functioned well throughout the test.

After restriking the pile, the center tube (which filled with fine soil during impact driving) was cleaned out to within approximately 0.6 m (2 ft) of the pile toe. Then, the gages and telltales were connected to an assembly plate that was lowered into the center tube, whereupon the center tube was grouted, whereupon the center tube was grouted, embedding the assembly plate and instruments.

Static Loading Test

The static loading test started on May 18, 1987, ten days after restriking. The test was performed by jacking against reaction beams connected to four reaction piles. The test arrangement was in general conformance with the ASTM D1143 and designed for a total reaction of 9,000 kN (1,000 tons). The test load was applied by means of four 2,700 kN (300-ton) hydraulic jacks each equipped with a load cell and spherical bearing plate leaving the jack pressure as backup. A gas-operated automatic load-holding system was used during the test.

The strain gage readings were read using a multichannel readout box. The pile head movement was measured by means of four Linear Variable Voltage Displacement

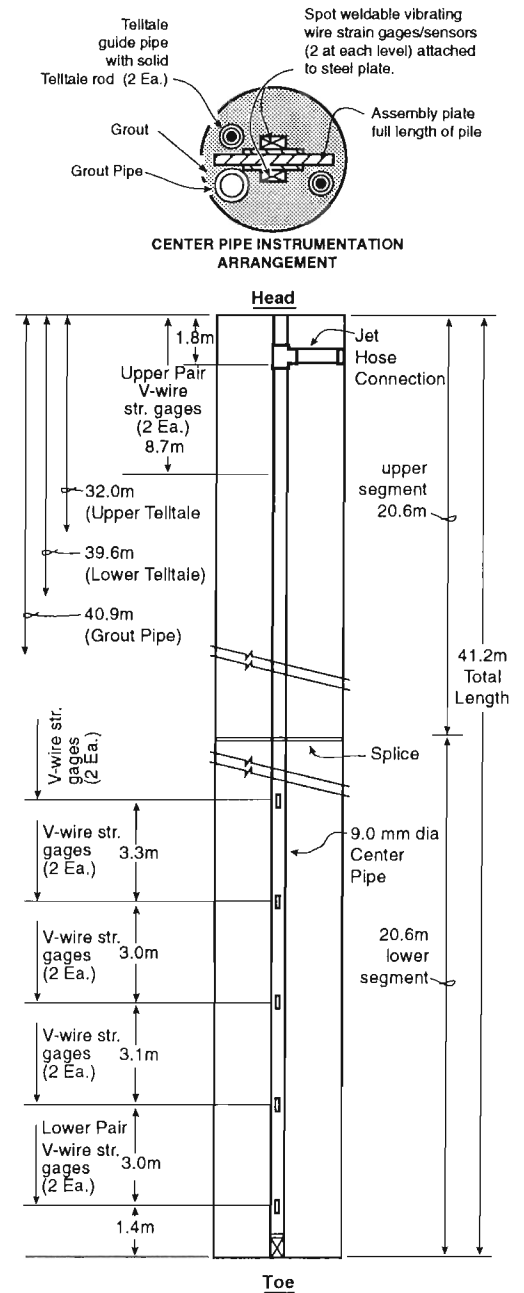


Fig. 3 Strain Gage and Telltale Arrangement

Transducers (LVDT's) arranged in diametrically opposed pairs. The telltales registered pile shortening and measurements were obtained by means of linear potentiometers. The movement gages were connected to a multichannel readout

box where the readings were displayed and recorded on a strip chart.

Load was applied to the test pile in 15-minute increments. The first 4,700 KN (525 tons) of load was applied to the test pile in increments of 670 KN (75 tons). Thereafter, the increments were 445 KN (50 tons) up to a load of 7,300 KN (825 tons). In attempting the next increment, the pile began to plunge and unloading started from the maximum load of 7,400 KN (831 tons).

DYNAMIC TEST RESULTS

During jetting, the pile penetrated the various soil strata with little difficulty. The jetting was terminated in the very dense sand layer, Stratum 3, and the pile was impact driven for the remainder of the installation depth.

The records taken during the impact driving are summarized on the pile driving diagram presented in Fig. 4. The diagram shows, for each 0.3 m (1 ft) of driving, the penetration resistance, PRES, the maximum transferred energy, EMAX, and the maximum force (impact), FMAX, at the pile head as the pile penetrated the dense sand, the medium stiff silt, and, eventually, into the siltstone bedrock.

Driving through the silt was very easy; the penetration resistance, PRES, was generally smaller than 12 blows/0.3 m, that is, smaller than

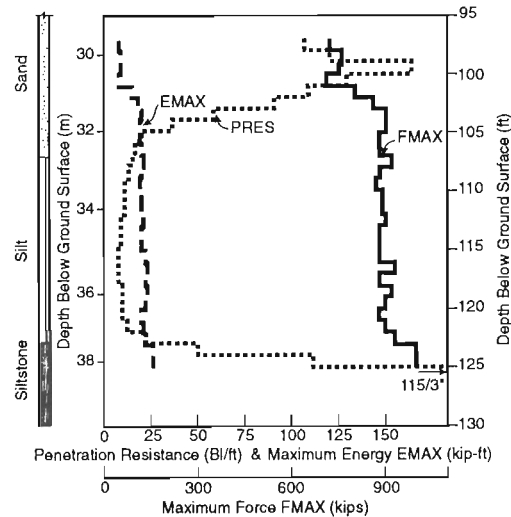


Fig. 4 Pile Driving Diagram

1 blows/25mm. When reaching the siltstone, the pile penetration resistance increased markedly. At EOID, the pile had penetrated about 0.6 m (2 ft) into the bedrock and the final PRES value was 38 blows/25mm. At restriking two days later, the equivalent PRES value was 90 blows/25mm, as determined for 58 blows.

Fig. 5 presents representative wave traces of force and velocity as recorded during the EOID and at RSTR. The EOID trace indicates little or no shaft resistance in the jetted zone and suggests the presence of a large toe quake before registering some compression toe reflection, that is, toe resistance. In contrast, the RSTR trace does not suggest a large quake and indicates more shaft resistance, that is, soil set-up has occurred. Still, only little shaft resistance is indicated in the jetted zone.

The data from the traces shown in Fig. 5 were analyzed by means of the CAPWAP program (Rausche et al., 1972). The CAPWAP calculated net toe and pile head movements compared well with the observed PRES values. The CAPWAP results are summarized in Table 2.

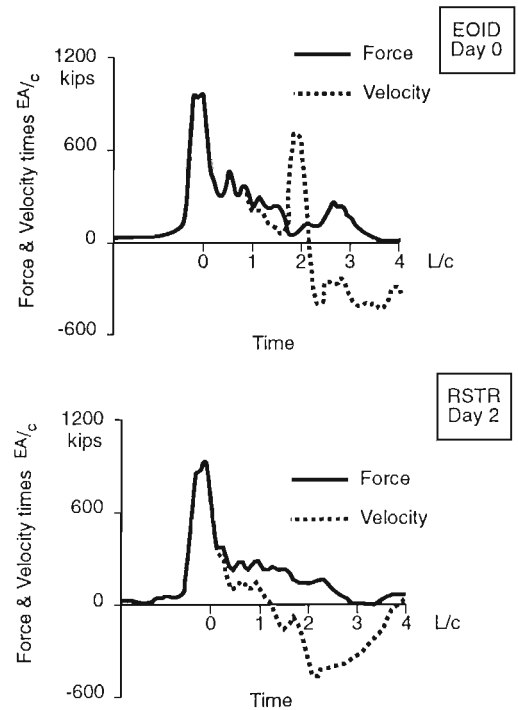


Fig. 5 Wave Traces at EOID and RSTR

TABLE 2. Summary of CAPWAP Computations

	RULT KN (ton)	SHAFT KN (ton)	TOE KN (ton)	TOE DISPL. mm (inch)
E OID	2,500 (280)	950 (107)	1,540 (173)	9.65 (0.38)
RSTR	3,250 (365)	2,040 (229)	1,210 (136)	5.59 (0.22)
Comb.	3,580 (402)	2,040 (229)	1,540 (173)	— —

The load distributions determined by CAPWAP are presented in Fig. 6. Because of the large quake at EOID, which was not overcome by the impact, and the small penetration per blow, the full toe resistance was not mobilized by the hammer impact. And, of course, at RSTR, the impact is not nearly mobilizing the pile toe capacity as evidenced by the even smaller toe movement.

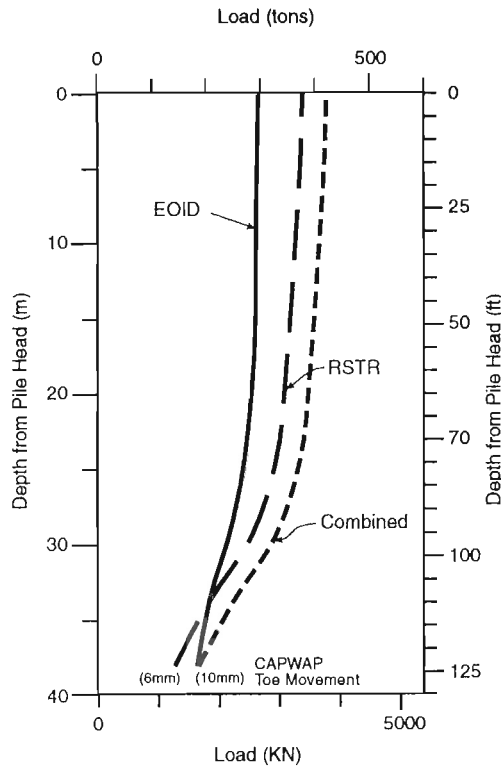


Fig. 6 CAPWAP Computed Load Distributions

Further, the slope of the load distribution curve at RSTR is steeper than at EOID, which indicates that the unit shaft resistance at RSTR is correspondingly larger than at EOID. Because of the increased shaft resistance due to soil set-up at RSTR, the hammer energy is less capable of mobilizing toe resistance and the calculated toe resistance at RSTR is smaller than at EOID. By combining the toe resistance at EOID with the shaft resistance at RSTR, a higher estimate of ultimate soil resistance is obtained; 3,600 KN (400 ton). However, also this upward adjusted value is clearly underestimating the pile capacity.

The soil set-up is the result of dissipation of the piling induced excess pore pressure in the soil after the initial driving. The two-day wait between EOID and RSTR is probably sufficient for allowing full consolidation of the sand layers. However, in the silt layer in Stratum 4, it is probable that the excess pore pressures are still dissipating. Therefore, the unit shaft resistance in the silt indicated by the slope of the load distribution curve at RSTR is smaller than the value expected after some further wait.

Further, the development of soil set-up occurs together with a build-up of residual load in the pile which combines with the residual load generated by the pile driving. The CAPWAP analysis is performed under the assumption that no residual load exists in the pile. The neglect of the residual load does not affect the computed total capacity. However, the assumptions lead to a computed shaft resistance that is larger than the actual. A corresponding error appears as an underestimation of the mobilized toe resistance.

STATIC TEST RESULTS

Failure Load

The main results of the static loading test are presented in Fig. 7, showing the load applied to the pile head plotted against the measured movement of the pile head and pile toe.

The maximum load is considered to be representative of the failure load—the capacity of the pile. The load-movement curve was analyzed to determine the Davisson Offset Limit, the BrinchHansen Failure Load, and the Chin Kondner Extrapolation Load (Fellenius, 1980; Canadian Foundation Engineering Manual, 1985; Fellenius and Rasch, 1990).

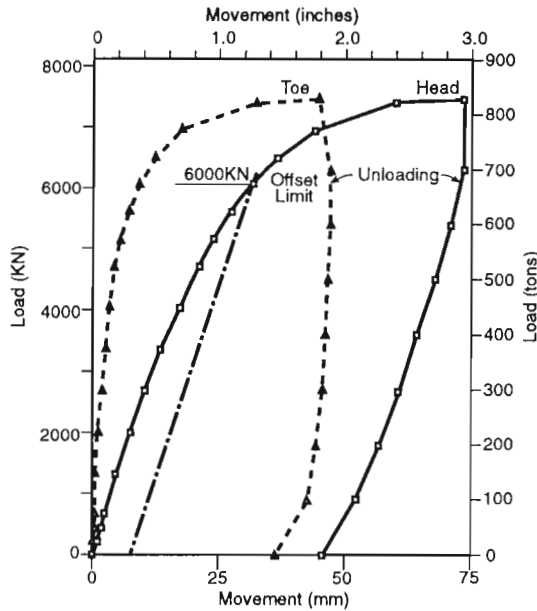


**Fig. 7 Load-Movement Diagram;
Pile Head and Pile Toe**

The Davisson Offset Limit Load is 6,000 KN (675 tons), well below the actual failure load. The BrinchHansen failure load is 7,500 KN (843 tons) occurring at a calculated pile head movement of 96 mm (3.8 inch) and it agrees well with the plunging failure. The Chin Kondner Extrapolation load is 8,300 KN (934 tons), a value of little relevance to the actual failure load. However, the BrinchHansen and Chin lines are consistent which indicates good quality test data.

The pile head movement at failure was 75 mm (2.94 inch), or 15 % of the pile face-to-face diameter, somewhat larger than the conventionally assumed movement value at failure of 5 % to 10 % of the diameter. (The 75-mm movement corresponds to 13 % of the pile equivalent diameter taken as the diameter of a circle with the same cross sectional area as the square pile).

The pile toe was forced a total of 45 mm (1.78 inch) into the siltstone. A penetration of the pile toe of 12 mm (0.49 inch) was obtained at the applied load of 6,450 KN (725 tons), whereafter only very little additional resistance was mobilized. The 12-mm pile toe movement corresponds to 2.5 % of the pile face-to-face diameter and to 2.2 % of the equivalent

diameter. (A toe movement equal to the CAPWAP computed quake at RSTR of about 5.6 mm—0.22 inch was reached at the applied load of 5,100 KN (575 tons).

Load Distribution

The strain gage and telltale data provide strain values for each applied load. These strain values are conventionally multiplied with the Young's modulus of the pile material to derive stress. However, with concrete piles, it is always difficult to determine the appropriate pile modulus value to use. Fellenius (1989) has indicated a numerical derivation method consisting of plotting the increment of load over the increment of strain versus the strain—the tangent modulus method. The values will plot in a straight line after all shaft resistance has been mobilized (assuming that the soil does not exhibit an appreciable strain softening). Fig. 8

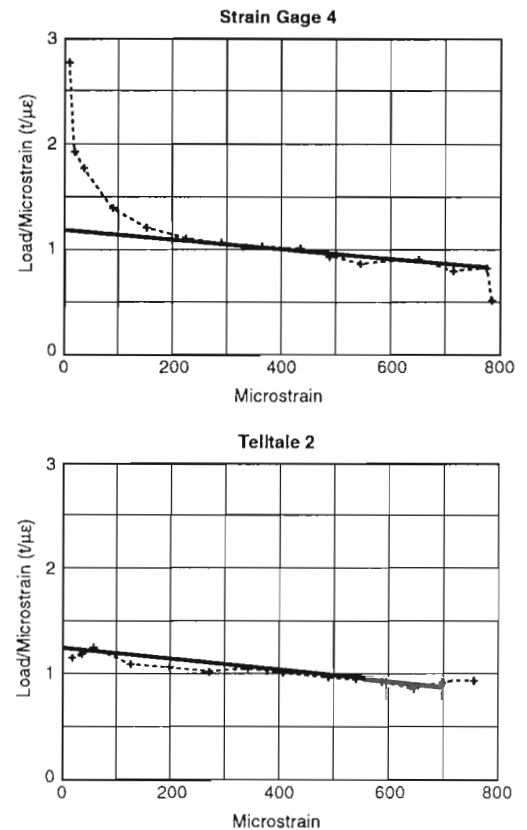


Fig. 8 Tangent Modulus versus Strain

presents this construction for one strain gage (Gage 4 at Depth 28 m; 91 ft) and one telltale (the short telltale, representative for the strain and stress at about half its length, i.e., Depth 15 m; 50 ft).

The diagram in Fig. 8 indicates that the pile material modulus is not constant with stress. Through linear regression of the sloping line (the tangent modulus line), the relation for stress and strain is determined from the data, as follows.

$$\sigma = 0.5 A \epsilon + B \epsilon$$

- where σ = stress
 ϵ = strain
A = slope of the line
B = y-intercept of line

By means of the tangent modulus construction, the stress-strain relations of the gage and telltale data were determined. Table 3 presents the results for strain-gage No. 4, showing that the concrete modulus does diminish with increasing strain. However, using a constant modulus would have caused only a negligible error, about 2 % over the range of the test.

The measured strains were used to calculate the load distribution in the pile for all the applied loads as presented in Fig. 9. The three oval symbols indicate the load determined from the telltales at the applied load of 825 tons (7,300 KN) plotted at midpoint of the telltale lengths. The lowest telltale datum point is determined from the difference of compression recorded by the short and long telltales. Its value is considerably less accurate than the values from the individual telltale lengths (because in subtracting the measurements of compression, the errors of the measurements are

TABLE 3. Stress-Strain Relations

AT A STRAIN OF (microstrain):		100	400	700
Tangent modulus	GPa	37.58	36.54	35.51
	ksi	5450	5300	5150
Secant modulus	GPa	37.75	37.23	36.71
	ksi	5475	5400	5325
Resulting stress	MPa	3770	14890	25710
	psi	548	2160	3730

combined and, then, the resulting error in the calculated strain is magnified by division with the smaller telltale length)

The thick, dash-dot line is the load distribution determined from a matching of the test data to an effective stress analysis (beta-method) (Goudreau and Fellenius, 1990). The match was obtained by assuming a hydrostatic distribution of pore pressure and assigning beta-coefficients of, only, 0.1 to the soils in the jetted zone, 0.3 to the dense sand immediately below, and 0.7 to both the silt and the mudstone combined with a toe bearing coefficient, N_t , of 25 at the 38 m (125 ft) depth.

As indicated in Fig. 9, very little shaft resistance was obtained in the jetted zone. In contrast, considerable shaft resistance is indicated below the end of the jetted zone at a depth of 30 m (97 ft) in dense sand, in the clayey silt starting at a depth of 32 m (107 ft), and, from 37 m (123 ft), in the siltstone. The analysis of the data from the lowest strain-gage pair, 1.4 m (4.5 ft) above the pile toe, indicates a maximum load of 3,000 KN (340 tons).

Fig. 10 presents a load-movement diagram obtained by plotting the load evaluated from the lowest strain-gage pair versus the telltale recorded toe movement. The diagram also includes the CAPWAP computed toe resistance

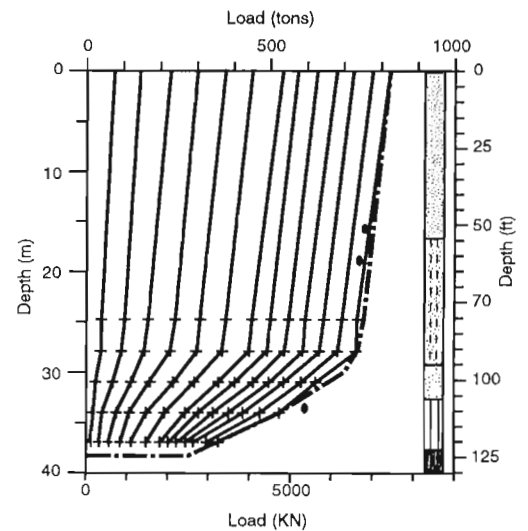


Fig. 9 Load Distributions Determined from analysis of Pile Instrumentation

plotted against the computed toe movement. The diagram does not compensate for the residual load at the toe of the pile.

DISCUSSION and CONCLUSIONS

The test results provide a basis for comparing estimates of pile capacity and load distribution determined from static and dynamic measurements. Many investigators have reported good to excellent correlation between static and dynamic estimates of total capacity. However, only little information has been published regarding the distribution between shaft and toe resistance, in particular with regard to the distribution of the shaft resistance along the pile. Seidel et al. (1988) reported a comparison between results from dynamic and static tests on an about 10 m (30 ft) long, prestressed concrete pile driven through alluvial sands and into a limestone. Dynamic tests were performed at EOID and at RSTR 7 days and 535 days after EOID giving capacities of 2,290 kN, 3,290 kN, and 4,120 kN (257 tons, 370 tons, 463 tons), respectively. The paper points out that, because the soil consisted of sand, the observed set-up between the 7-day and the 535-day tests was not anticipated. (Continued increase of strength and capacity in sand is not a unique phenomenon, however, as

shown by Schmertmann, 1991). The load distributions determined in static loading tests on three instrumented piles and by CAPWAP analysis of RSTR blows on the same piles showed an excellent agreement.

Holloway and Romig (1988) reported a fair agreement between CAPWAP results, static tests, and CPT estimation of load distribution for a 20 m (70 ft) long test pile driven in alluvial cohesive and non-cohesive soils.

The load distribution determined from the test data have been compiled for comparison in Fig. 11. The comparison shows clearly that (1) for both the CAPWAP and the static analyses only very little shaft resistance occurred in the jetted zone, (2) the shaft resistance below the jetted zone was much smaller in the CAPWAP analysis than in the static analysis suggesting incomplete soil set-up at the time of restriking, and (3) the toe resistance mobilized in the CAPWAP at a toe movement of about 6 mm (0.22 inch) is much smaller than the toe resistance mobilized in the static loading test.

It is therefore likely that the unit shaft resistance below the jetted zone continued to increase beyond the first two days after EOID.

As previously discussed, the pile was not free of stress at the start of the static loading test, but

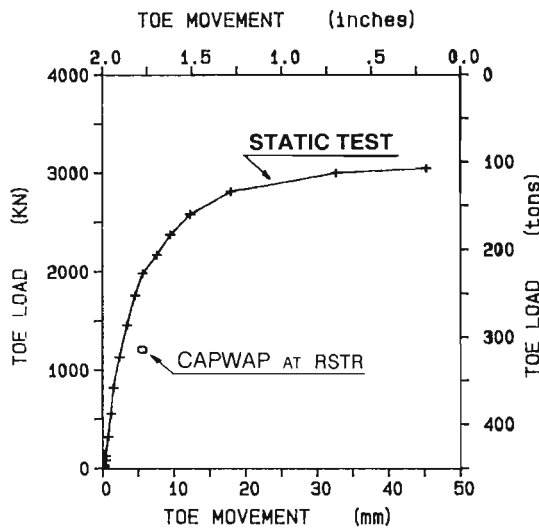


Fig. 10 Pile Toe Load-Movement Diagram

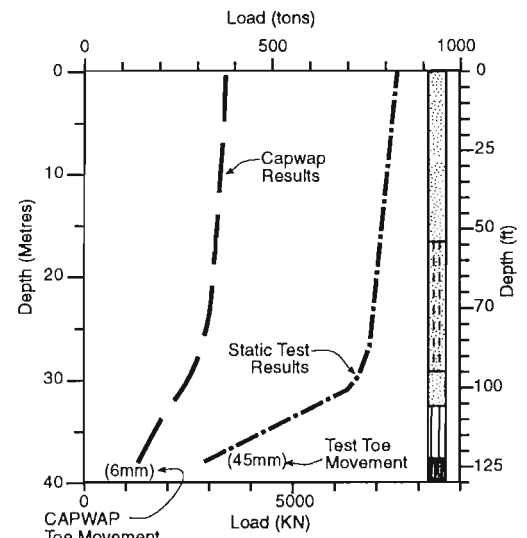


Fig. 11 Comparison of Load Distributions from CAPWAP Analysis and Static Test

subjected to residual load. Therefore, the high beta-coefficient value of 0.7 used to match the static analysis to the test data is apparent, only, and includes the effect of residual load. Judging from load distribution determined in the analysis of the strain-gage data, it is probable that the maximum residual load occurs at the pile toe, which simplifies the estimation of its magnitude and distribution. (For aspects of determining residual load, see Fellenius, 1991; Altaee et al., 1992). Therefore, the corrected beta-coefficient is closer to half the indicated value, that is, about 0.35 in the silt and siltstone, and the correct toe resistance at failure is about 560 tons (5,000 KN). The corresponding toe bearing coefficient is about 50. The balance, 2,400 KN (270 tons), to the failure load is then the shaft resistance corrected for residual load.

As evaluated from the test data and analyses, the ultimate shaft resistance is estimated to a value of about 2,400 KN (270 tons). Because (in the long-term situation) the neutral plane will be very close to the pile toe, all or almost all of the shaft resistance will become negative skin friction and, therefore, the dragload to consider for the structural strength of the pile is about equal to the ultimate shaft resistance found in the test.

As a result of the test and the analyses, a maximum design load of 2,670 KN (300 tons) was recommended for similar concrete piles driven into the siltstone. This value includes aspects of limiting settlement and the structural compressive stresses at the neutral plane.

REFERENCES

ALTAEE, A., FELLENIUS, B. H., and EVGIN, E., 1992. Axial load transfer for piles in sand. I: Tests on an instrumented precast pile. 43rd Canadian Geotechnical Conference, Quebec City, October 1990, Canadian Geotechnical Journal, Vol. 29, No. 1.

FELLENIUS, B. H., 1980. The analysis of results from routine pile loading tests. Ground Engineering, London, Vol. 13, No. 6, pp. 19 - 31.

CANADIAN FOUNDATION ENGINEERING MANUAL, 1985. Second Edition. Part 3: Deep Foundations. Canadian Geotechnical Society, Technical Committee on Foundations, BiTech Publishers, Vancouver, 460 p.

FELLENIUS, B. H., 1989. Tangent modulus of piles determined from strain data. The American Society of Civil Engineers, ASCE, Geotechnical Engineering Division, the 1989 Foundation Congress, F. H. Kulhawy, Editor, Vol. 1, pp. 500 - 510.

FELLENIUS, B. H. and RASCH, N. C., 1990. Failpile Version 1.1 Users Manual, Bengt Fellenius Consultants Inc., Ottawa, 38 p.

FELLENIUS, B. H., 1991. Results of Foundation Engineering Congress pile loading tests. American Society of Civil Engineers, ASCE, Journal of Geotechnical Engineering, Vol. 117, No. 1, pp. 188 - 191.

GOUDREAU, P. A. and FELLENIUS, B. H., 1990. Unipile Version 1.0 Users Manual, Bengt Fellenius Consultants Inc., Ottawa, 76 p.

HOLLOWAY, D. M. and ROMIG, G. A., 1988. CPT and dynamic testing in foundation design—A case history. Proceedings of the Third International Conference on the Application of Stress-Wave Theory to Piles, Ottawa, May 25 - 27, 1988, pp. 889 - 901.

RAUSCHE, F., MOSES, F., and GOBLE, G. G., 1972. Soil resistance predictions from pile dynamics. American Society of Civil Engineers, ASCE, Journal of Soil Mechanics and Foundation Engineering, Vol. 98, SM9, pp. 917 - 937.

RAUSCHE, F., GOBLE, G. G., and LIKINS, G. E., 1985. Dynamic determination of pile capacity. American Society of Civil Engineers, ASCE, Journal of Geotechnical Engineering, Vol. 111, GT3, pp. 367 - 383.

SEIDEL, J. P., HAUSTORFER, I. J., and PLESIOITIS, S., 1988. Comparison of dynamic and static testing for piles founded into limestone. Proceedings of the Third International Conference on the Application of Stress-Wave Theory to Piles, Ottawa, May 25 - 27, 1988, pp. 717 - 723.

SCHMERTMANN, J. H., 1991. The mechanical aging of soils. American Society of Civil Engineers, ASCE, Journal of Geotechnical Engineering, Vol. 117, No. 9, pp. 1288 - 1330.